NeuroImage: Clinical 32 (2021) 102791

Contents lists available at ScienceDirect

NeuroImage: Clinical

journal homepage: www.elsevier.com/locate/ynicl

Premotor and fronto-striatal mechanisms associated with presence hallucinations in dementia with Lewy bodies

Nicolas Nicastro [a,d,1,*], Giedre Stripeikyte [b,c,1], Frédéric Assal [a,d], Valentina Garibotto [d,e], Olaf Blanke [a,b,c]

[a] Division of Neurology, Department of Clinical Neurosciences, Geneva University Hospitals, Geneva, Switzerland
[b] Center for Neuroprosthetics, Swiss Federal Institute of Technology (EPFL), Geneva, Switzerland
[c] Brain Mind Institute, Faculty of Life Sciences, Swiss Federal Institute of Technology (EPFL), Lausanne, Switzerland
[d] Faculty of Medicine, University of Geneva, Switzerland
[e] Division of Nuclear Medicine, Geneva University Hospitals, Geneva, Switzerland

ARTICLE INFO

Keywords:
Dementia
Psychosis
Hallucinations
Brain metabolism
Dopamine

ABSTRACT

Introduction: presence hallucinations (PH) are frequent in dementia with Lewy bodies (DLB), but their cortico-subcortical origin is unknown. Recent studies have defined key frontal and temporal areas contributing to the occurrence of PH (PH-network) and tested their relevance in subjects with Parkinson's disease (PD). With the present study, we aimed at disentangling the metabolic and dopaminergic correlates of pH as well as their relation to a recently defined PH brain network in DLB.

Methods: for the present study, we included 34 DLB subjects (10 with PH (PH +); 24 without PH (PH-)), who underwent ^{18}F-FDG PET and ^{123}I-FP-CIT SPECT imaging. We performed ^{18}F-FDG PET group comparisons, as well as interregional correlation analyses using ^{18}F-FDG PH-network regions as a seed.

Results: PH + versus PH- had reduced ^{18}F-FDG uptake in precentral, superior frontal and parietal gyri, involving ventral premotor cortex (vPMC) of the PH-network that showed strongly reduced functional connectivity with bilateral cortical regions. ^{18}F-FDG vPMC uptake was negatively correlated with caudate ^{123}I-FP-CIT uptake in PH+ ($p = 0.028$) and interregional correlation analysis seeding from the vPMC showed widespread fronto-parietal ^{18}F-FDG decreases in PH + .

Discussion: these findings uncover the pivotal role of vPMC (involved in a PH-network) and its cortico-striatal connections in association with PH in DLB, improving our understanding of psychosis in neurodegeneration.

1. Introduction

Dementia with Lewy bodies (DLB) is the second most common degenerative dementia after Alzheimer's disease (AD), accounting for 15% of cases (Vann Jones and O'Brien, 2014). It is defined by a progressive cognitive decline interfering with the activities of daily living, in association with core clinical features of parkinsonism, visual hallucinations (VH), cognitive fluctuations and REM sleep behaviour disorder (McKeith et al., 2017). Hallucinations and other psychotic symptoms have a particular clinical relevance, as they are highly prevalent in DLB as compared to AD and other neurodegenerative disorders (Gomperts, 2016; Mosimann et al., 2006). Therefore, the presence of VH or PH in subjects with cognitive impairment may improve the diagnostic accuracy of DLB and allow specific treatment recommendations (e.g. avoiding antipsychotic drugs). The most common hallucinations in DLB patients are encountered in the visual modality and putative pathophysiological changes include decreased posterior brain metabolism, as well as altered attentional and visual networks (Sala et al., 2019; Morbelli et al., 2019; Imamura et al., 1999; O'Brien et al., 2005; Perneczky et al., 2008). Yet, hallucinations in other modalities, as well as misidentification syndromes and delusions, are also commonly described in DLB, although much less is known about their underlying brain mechanisms (Ballard et al., 1999; Nagahama et al., 2007).

One common neuropsychiatric feature frequently encountered in DLB is presence hallucination (PH), also being termed *sense of presence* or *feeling of presence*. PH is defined as the vivid sensation that somebody

* Corresponding author.
E-mail address: nicolas.nicastro@hcuge.ch (N. Nicastro).
[1] These authors contributed equally to the manuscript

https://doi.org/10.1016/j.nicl.2021.102791
Received 16 March 2021; Received in revised form 11 August 2021; Accepted 13 August 2021
Available online 23 August 2021

is nearby when no one is actually present and can neither be seen nor heard. To the best of our knowledge, only two studies have to date investigated the brain mechanisms of pH in DLB (Nagahama et al., 2010);(Nicastro et al., 2020). Using ^{99m}Tc-hexamethyl propyleneamine oxime (HMPAO) single photon emission computed tomography (SPECT), Nagahama *et al.* reported hypoperfusion of the ventral occipital gyrus and parietal areas in association with a symptom cluster grouping PH and VH (Nagahama et al., 2010). On the other hand, Nicastro *et al.* analyzed PH alone, using ^{18}F-fluorodeoxyglucose (FDG) positron emission tomography (PET) and described reduced metabolism in fronto-parietal areas (Nicastro et al., 2020).

PH also occur in other neurological conditions and have classically been linked to alterations of the body schema (Lopez et al., 2008). Fenelon and others showed that PH are frequent in patients with Parkinson's disease (PD) (Fenelon et al., 2011; Lenka et al., 2019; Ffytche et al., 2017) and may occur in recurrent fashion(Fenelon et al., 2011), affecting approximately 50% of patients with PD(Fenelon et al., 2011; Lenka et al., 2019; Ffytche et al., 2017; Wood et al., 2015) and often precede the onset of structured VH (Marinus et al., 2018). Based on PH that were induced by electrical stimulation of a cortical region involved in sensorimotor processing (Arzy et al., 2006) and associated sensorimotor symptoms in neurological patients with PH, a robotic method was recently designed to safely induce PH in healthy participants using controlled sensorimotor stimulation (Blanke et al., 2014). Recently, this technique was applied to PD patients (Bernasconi et al., 2021), revealing that those with symptomatic PH (versus patients without PH) were characterized by abnormally heightened sensitivity to sensorimotor stimulation. The study also identified a cortical network for PH (PH-network) including the posterior superior temporal sulcus region (pSTS), inferior frontal gyrus (IFG), and ventral premotor cortex (vPMC). This was based on robot-induced PH and functional MRI (fMRI) in healthy subjects and lesion network analysis (resting state functional connectivity data) in neurological (non-parkinsonian) patients with focal brain lesion (i.e. stroke, tumor) experiencing symptomatic PH. The study also reported that the PH-network was selectively altered in PD patients with PH and this alteration was further associated with cognitive impairment (Bernasconi et al., 2021).

Based on these recent data, we here applied our recently defined PH-network approach to DLB patients with and without PH in order to investigate potential abnormalities of the PH-network and to assess its relationship with nigrostriatal pathways. More specifically, we used ^{18}F-FDG PET data to compare brain glucose metabolism within the PH-network across groups, assessed connectivity of the PH-network areas to the whole brain, and determined its association with presynaptic dopaminergic density using ^{123}I-FP-CIT SPECT. Considering our previous work on DLB subjects with symptomatic PH, as well as the brain network of robot-induced PH in healthy controls and PD subjects, we aimed at investigating the involvement of the latter brain network in DLB patients with PH as compared to DLB patients without PH. Another objective was to disentangle the metabolic and dopaminergic neural correlates of pH in DLB.

Based on previous research, we expected the following: a reduced ^{18}F-FDG PET uptake in fronto-parietal areas for DLB subjects experiencing PH, and a disruption of the PH-network involving frontal cortex in PH + subjects. Considering mixed results regarding the association between ^{123}I-FP-CIT imaging and PH in degenerative parkinsonisms, we also assessed whether striatal dopaminergic uptake was associated with PH-network impairment.

2. Material and methods

2.1. Participants

This retrospective study was conducted in compliance with the declaration of Helsinki and received an approval from our local Ethics Committee (study protocol NAC 12-026R, Canton of Geneva, Switzerland). We considered all subjects who underwent both ^{123}I-FP-CIT SPECT and ^{18}F-FDG PET scans between October 2003 and October 2019 at Geneva University Hospitals, Switzerland using the same acquisition and image processing protocols. We collected clinical data (age, sex, disease duration), in addition to mini-mental state examination (MMSE) and levodopa equivalent daily dosage (LEDD). All patients had a clinical diagnosis of probable DLB according to the most recent consensus criteria (McKeith et al., 2017). A clear reduction of striatal ^{123}I-FP-CIT uptake was observed for all included patients, confirming the presence of a degenerative condition. In addition, a typical pattern of posterior ^{18}F-FDG hypometabolism was noted for all included subjects.

Based on the information gathered in the medical file, PH prevalence was collected by an experienced clinician (N.N). As a core clinical criterion for DLB, the co-occurrence of well-formed VH was also assessed using a non-standardised questionnaire. These symptoms were assessed during the initial neurological evaluation which then led to PET and SPECT imaging, and the subsequent confirmation of a diagnosis of probable DLB.

2.2. Image acquisition and pre-processing

^{18}F-FDG PET. Subjects received 250 MBq of ^{18}F-FDG in slow IV injection under standardized conditions (supine position, low ambient noise, dim roomlight, eyes open). Usual medication was continued before and on the day of scan. PET/CT data acquisition was performed on a Biograph tomograph (Siemens Healthcare, Erlangen, Germany) using manufacturer's recommendations and according to the European Association of Nuclear Medicine Neuroimaging Committee (Varrone et al., 2009). PET acquisition started approximately 30 min after ligand injection. CT study was used for attenuation and scatter correction, then followed by PET emission study (20 min). We used ordered-subset-expectation–maximisation (OSEM) algorithm for image reconstruction.

^{18}F-FDG-PET brain images were pre-processed using Statistical Parametric Mapping (SPM12, fil.ion.ucl.ac.uk/spm/) running in MATLAB R2019b Version 9.6 (MathWorks Inc., Sherborn, MA, USA). First, manual image reorientation and positioning to a structural (T1) MRI template from SPM12 was performed. Images were then normalized into Montreal Neurological Institute (MNI) space, resampled to a 2x2x2 mm^3 voxel size and smoothed with an 8 mm^3 full-width at half maximum (FWHM) Gaussian kernel.

^{123}I-FP-CIT SPECT. Patients received 185 MBq of ^{123}I-FP-CIT (ioflupane, DaTSCAN®, GE Healthcare, Glattbrug, Switzerland) in slow IV injection and Lugol solution (or sodium perchlorate) was used for thyroid blockade. SPECT imaging was performed according to the manufacturer's instructions and was acquired 4 h after ioflupane injection, using the same triple-head gamma camera (GCA-9300A/UI Toshiba Medical Systems AG, Oetwil am See, Switzerland) equipped with fan beam low-energy high-resolution collimators. Details of the acquisition and preprocessing are available in (Nicastro et al., 2016).

2.3. Regions of interest

PH-network (Figure S1) areas as defined in (Bernasconi et al., 2021) were used as regions of interest (ROIs). PH-network was defined in a previous study as a cluster of brain regions whose impairment was associated with both robot-induced PH in healthy participants and symptomatic PH in neurological patients (for more details see [22]). The PH-network included bilateral posterior superior temporal sulcus (pSTS; $x = \pm 54$, $y = -54$, $z = 0$), inferior frontal gyrus (IFG; $x = \pm 51$, $y = 18$, $z = 29$) and ventral premotor cortex (vPMC; $x = \pm 26$, $y = -18$, $z = 57$). Those areas were co-registered to the structural (T1) MRI template from SPM12 to match the normalized ^{18}F-FDG-PET image resolution.

2.4. Statistical analyses

Between-group analyses for demographics and clinical data were

performed with STATA Version 14.2 (College Station, TX, USA). Continuous variables were assessed for normality with Shapiro-Wilk test and plotted histograms. Between-group comparisons were performed with *t*-test or Mann-Whitney *U* test, accordingly. χ^2 test was used for discrete variables.

Whole-brain analysis. Whole-brain analyses were performed in SPM12, using a two-sample *t*-test design (PH + vs PH- groups) with Analysis of Covariance (ANCOVA) including age and sex as covariates. Individual pontine metabolism was used for intensity normalization as it has been shown not to be affected in subjects with dementia (Borghammer et al., 2008);(Minoshima et al., 1995) . Obtained T-maps were reported with an uncorrected threshold $p < 0.001$ peak level and minimum cluster extent (k) of 50 voxels. The reported brain areas are based on the automated anatomical labelling (AAL) atlas (Destrieux et al., 2010). Similar analyses were performed to compare DLB patients splitting depending on the absence or presence of VH.

ROI analysis. Mean ^{18}F-FDG uptake for each PH-network ROI (left and right vPMC, pSTS and IFG) were extracted using Marsbar (http://marsbar.sourceforge.net/index.html) toolbox for MATLAB and subjected to statistical analysis in R (R-project.org/). First, glucose uptake of these ROIs was normalized with the individual ^{18}F-FDG uptake in the pons. Glucose uptake within the PH-network was analysed using linear mixed-effects model with a Group (PH+, PH-) and PH-network ROIs (6 ROIs) as fixed effects and Subjects as a random effect. Post-hoc analyses for the between-group differences were performed using a significance threshold of false discovery rate (FDR) $p < 0.05$ correction. Subjects' age, sex and mean ^{18}F-FDG uptake in the pons were included as covariates of no interest. The same analysis of glucose uptake within the PH-network were performed by comparing VH + and VH- groups. For that purpose, power analysis was performed using G*Power software version 3.1.9.7. (Heinrich Heine Universität Dusseldorf, Germany) (Faul et al., 2007). We computed a multiple linear regression with effect size $f^2 = 0.35$ and α error probability = 0.05, which resulted in a critical sample size of n = 33.

Seed-to-whole-brain analysis. Interregional correlation analysis (IRCA) (Lee et al., 2008) was performed for both groups (PH+, PH-) separately using extracted and normalized mean ^{18}F-FDG uptake from the affected PH-network seeds as a covariate. IRCA analysis allows to observe regions presenting significant voxel-wise correlations with the seed region. The results were reported with an uncorrected threshold at $p < 0.001$ peak level and $k > 50$ voxels.

2.5. SPECT data analysis

^{123}I-FP-CIT SPECT striatal binding ratios (SBR) were obtained using the formula $(Uptake_{ROI} - Uptake_{Reference}) / Uptake_{Reference}$. ROIs used were left and right caudate nucleus and putamen, with the occipital lobe as a reference region.

Correlations. Pearson's correlations were performed between the mean striatal (bilateral caudate nucleus and putamen) dopamine SPECT uptake and mean ^{18}F-FDG uptake in affected PH-network ROI for each group. To further explore the performed correlations, a mediation analysis was conducted (for more details see supplementary information).

3. Results

3.1. Clinical characteristics of included subjects

Between October 2003 and October 2019, 1′896 subjects underwent ^{123}I-FP-CIT SPECT in our institution, including 112 subjects with a diagnosis of probable DLB. Of these, 34 subjects also had ^{18}F-FDG PET imaging and were therefore included in the present study. Demographics and baseline characteristics are available in Table 1. 10 DLB subjects had PH (PH +), while 24 did not experience PH (PH-). Regarding the PH + subjects, 7 felt a presence on one side of their body (1 on the left, 2 on the right, 4 on either side) and 3 behind their body. Both groups were comparable in terms of age, male/female distribution, MMSE and LEDD score, as well as prevalence of concomitant VH and ^{123}I-FP-CIT striatal uptake (all $p > 0.2$).

Table 1
Demographics and clinical data of included subjects.

	DLB – PH+ (n = 10)	DLB – PH- (n = 24)	P
Age, years	71 ± 6.9	74 ± 6.7	0.2*
Sex (Male/Female)	6/4	15/9	0.8$
Education, years	13.3 ± 2.5	12.5 ± 3.4	0.6*
Disease duration, years	1.5 ± 1.4 (0.5 – 4)	1.2 ± 0.8 (0.25 – 3)	0.79#
MMSE	22.2 ± 5.4	21.5 ± 4.3	0.8#
MDS-UPDRS III	12.1 ± 12.9	13.8 ± 12.1	0.45#
LEDD (mg)	119 ± 271 (0 – 800)	90 ± 149 (0 – 400)	0.76#
Visual hallucinations	7/10 (70%)	13/24 (54%)	0.39$
Mean caudate nucleus ^{123}I-FP-CIT uptake	1.43 ± 0.37	1.64 ± 0.66	0.36*

Demographics and clinical characteristics of DLB patients with and without PH included in the study. Abbreviations: MMSE – mini-mental state examination; LEDD – levodopa equivalent daily dosage (in mg), MDS-UPDRS III – Movement Disorders Society Unified Parkinson Disease Rating Scale, part III. Values are mean ± standard deviation (range). * = *t*-test, $ = Chi-squared test, # = Mann-Whitney *U* test

3.2. Whole-brain ^{18}F-FDG PET between-group comparisons

PH + showed a significant reduction of ^{18}F-FDG uptake compared to PH- in left superior parietal gyrus and precentral gyrus, as well as bilateral superior frontal gyrus (Fig. 1). In addition, we observed increased ^{18}F-FDG uptake for PH + group in right middle frontal gyrus, left cerebellum, and medulla (Table 2) ($p < 0.001$, $k = 50$ voxels). Of note, no significant differences in terms of ^{18}F-FDG uptake was observed between VH+ (n = 20) and VH- (n = 14) groups ($p > 0.001$).

3.3. ^{18}F-FDG PET within the PH-network

Regarding the recently described PH-network (Bernasconi et al., 2021), we observed a significant Group × ROI interaction ($F_{(5,160)} = 3.9p = 0.002$), implying that there were distinct ^{18}F-FDG uptake differences between PH + and PH- groups.

The interaction was driven by a significant ^{18}F-FDG uptake reduction in the left vPMC of the PH-network ($t = -2.8$, $p = 0.047$) for PH+ ($M = 1.19 \pm 0.13$, 95% confidence interval (CI) = [1.09, 1.29]) compared to PH- ($M = 1.32 \pm 0.15$, CI(95%) = [1.26, 1.39]) (Fig. 2A). Left vPMC of the PH-network ROI spatially overlapped with the main cluster of reduced ^{18}F-FDG uptake cluster in PH + observed in whole-brain analysis (Fig. 2B). No other region of the PH-network showed significant differences between PH + and PH- groups (Figure S2). We did not observe a main effect of Group (PH+: $M = 1.32 \pm 0.19$, CI(95%) = [1.27, 1.37], PH-: $M = 1.32 \pm 0.18$, CI(95%) = [1.29, 1.35], $F_{(1,29)} = 1.0$, $p = 0.32$), suggesting that ^{18}F-FDG uptake did not differ globally for the entire PH-network. Finally, there was a predicted main effect of ROI ($F_{(5,160)} = 20$, $p < 0.0001$), showing that ^{18}F-FDG uptake varied between the different ROIs of the PH-network, but independently of the group. Clinical covariates did not show any significant effects (Age: $F_{(1,29)} = 0.02$, $p = 0.87$; Sex: $F_{(1,29)} = 0.2$, $p = 0.6$; Pontine ^{18}F-FDG uptake: $F_{(1,29)} = 4.2$, $p = 0.06$).

Additional analysis regarding VH was performed with the same PH-network but defining two different patient groups based on the occurrence of VH (VH + and VH- groups, Figure S3). This analysis revealed no significant main effect of Group ($F_{(1,29)} = 1.8$, $p = 0.18$) nor a Group × ROI interaction ($F_{(5,160)} = 0.56p = 0.72$), showing that none of the six PH-network regions (including left vPMC) differed between both VH-

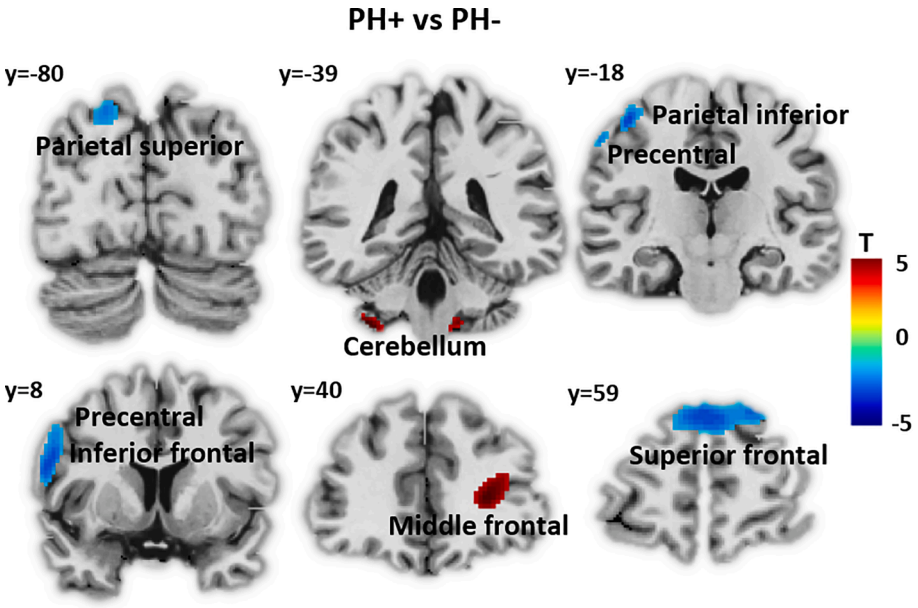

Fig. 1. Whole brain analyses: PH + vs. PH-. ^{18}F-FDG uptake comparison between patients with presence hallucination (PH +) and without (PH-). Lower ^{18}F-FDG uptake for PH + is depicted in blue. Higher ^{18}F-FDG uptake in PH + is shown in red (statistical threshold uncorrected $p < 0.001$, $k = 50$ voxels). (For interpretation of the references to colour in this figure legend, the reader is referred to the web version of this article.)

Table 2
Significant clusters for whole-brain between-group ^{18}F-FDG uptake
Regional clusters showing significant differences in 18F-FDG uptake between PH + and PH- patients. Statistical threshold uncorrected $p < 0.001$ with $k = 50$ voxels. X Y Z – stereotactic coordinates in Montreal Neurological Institute (MNI) space; T – SPM T-score; BA – Brodmann area, k – cluster size in voxels.

BA	Anatomical Label		k	Peak voxelMNI coordinate x	y	z	T
	PH+ > PH-						
	Cerebellum 8	L	79	−36	−40	−50	4.52
32	Middle frontal	R	252	26	40	10	4.21
	Medulla		61	0	−34	−58	3.92
	PH+ < PH-						
6, 4	Precentral,Postcentral	L	223	−38	−14	60	−4.95
9, 10	Medial superior frontal	L/R	426	2	62	32	−4.42
2, 4	Postcentral	L	79	−60	−22	48	−4.37
9, 44, 6	Precentral, Opercular part of inferior frontal	L	250	−56	8	26	−4.34
7, 19	Superior occipital, Parietal superior	L	86	−20	−80	44	−3.90

groups. Again, we observed a significant main effect of ROI, showing that connectivity differs across brain regions, independently of group ($F_{(5,160)} = 19.5$, $p < 0.0001$). Covariates of no interest did not show significant effects either (Age: $F_{(1,29)} = 0.02$, $p = 0.87$; Sex: $F_{(1,29)} = 0.2$, $p = 0.6$; Pontine ^{18}F-FDG uptake: $F_{(1,29)} = 4.2$, $p = 0.06$).

3.4. Between-group distinct ^{18}F-FDG connectivity seeding from vPMC (IRCA)

Using left vPMC as a seed region, we observed that PH + connectivity showed a significant positive correlation between left vPMC and bilateral caudate nucleus, and a significant negative correlation with the midbrain (Fig. 3A, Table 3). The PH- group showed a dramatically different pattern as our analysis revealed strong positive correlations between left vPMC and widespread cortical regions, centring on bilateral superior, middle, and inferior frontal gyri, premotor and precentral regions, as well as bilateral superior parietal lobule and right angular gyrus. Bilateral superior and middle temporal gyrus and cerebellum were also correlated (Fig. 3B, Table 3). No significant correlation was observed between the left vPMC and the striatum for PH-.

3.5. Correlations between ^{18}F-FDG PH-related network and striatal ^{123}I-FP-CIT SPECT

As we observed a significant between-group difference in left vPMC ^{18}F-FDG uptake (see Fig. 2A), we further explored its correlation with striatal ^{123}I-FP-CIT uptake in both PH-groups. For PH+, we observed a significant negative correlation with ^{123}I-FP-CIT SPECT uptake in the left caudate nucleus ($r = -0.69$, $p = 0.027$) (Fig. 4). No significant findings were observed for PH- (all $p > 0.6$, Table S2). Mediation analysis accounting for ^{18}F-FDG uptake of the midbrain did not show any significant effect ($p = 0.2$) (Figure S4, more details in supplementary information). There was no significant difference regarding between-group striatal ^{123}I-FP-CIT uptake ($p = 0.36$ for mean caudate nucleus, $p = 0.23$ for mean putamen).

4. Discussion

We observed the following three main findings in DLB patients with PH: (i) compared to PH-, PH + DLB patients had reduced brain glucose metabolism in fronto-parietal areas that especially involved the vPMC of the independently defined PH-network and (ii) showed functional connectivity changes of the vPMC with bilateral cortical regions that were drastically reduced for PH + . (iii) While metabolism of vPMC with the caudate nucleus was the only area positively correlated for PH + subjects, we observed a negative correlation between vPMC metabolism and the density of dopamine transporters in the caudate nucleus.

Using whole-brain ^{18}F-FDG PET, we demonstrated that PH + had lower uptake in the left prefrontal and premotor as well as in superior parietal regions (Fig. 1). These findings corroborate previous observations from our team using a partially overlapping group of DLB subjects (Nicastro et al., 2020). They are also in keeping with Blanke *et al.* (Blanke et al., 2014), who observed that interference with superior parietal cortex in patients suffering from focal brain damage and epilepsy is associated with PH. The major aim of the present study was to

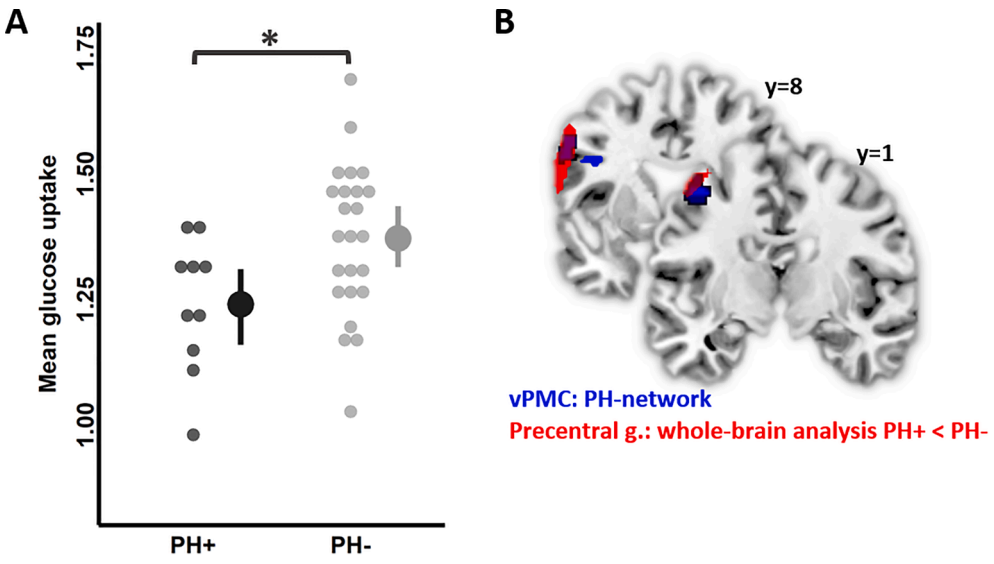

Fig. 2. . Between-group comparisons of ^{18}F-FDG uptake within PH-network area. (A) Mean ^{18}F-FDG uptake with 2.5% and 97.5% confidence interval bars of the left ventral premotor cortex (vPMC), PH-network area, in both groups. Left vPMC showed reduced ^{18}F-FDG uptake in PH + patients (black) compared to PH- patients (grey). Dots represent individual mean values. *$p < 0.05$ FDR corrected for multiple comparisons. (B) Left vPMC (dark blue) of PH-network overlapping with the left precentral gyrus (red) observed during whole-brain analysis. The cluster depicted in red had lower ^{18}F-FDG uptake in PH + patients compared to PH-. (For interpretation of the references to colour in this figure legend, the reader is referred to the web version of this article.)

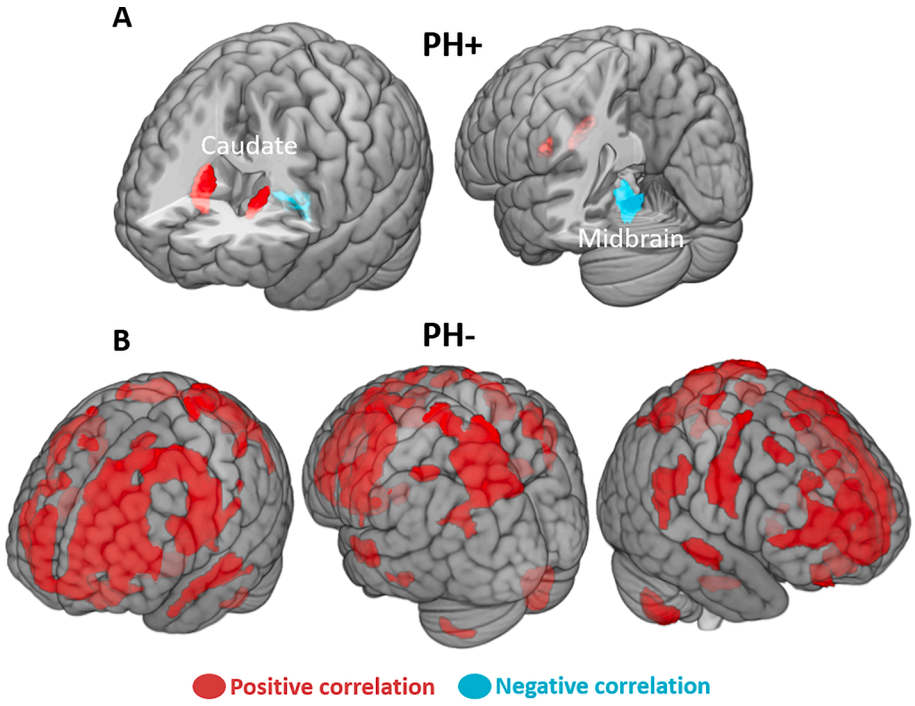

Fig. 3. ^{18}F-FDG uptake interregional correlation analysis (IRCA) using left vPMC as a seed region. IRCA using the left ventral premotor cortex (vPMC) as a seed for (A) PH + patients showing positive correlations with bilateral caudate nucleus (red) and negative correlation with the midbrain (blue); (B) PH- patients showing cortical widespread positive correlations (red). Statistical threshold uncorrected $p < 0.001$, $k = 50$ voxels. (For interpretation of the references to colour in this figure legend, the reader is referred to the web version of this article.)

investigate whether DLB patients with PH would show abnormalities in a recently defined PH-network. Within this PH-network, we observed a single region characterized by lower ^{18}F-FDG metabolism for the PH + DLB patients: left vPMC (Fig. 2). Overlap analysis showed that this region coincided with the cluster in vPMC determined by whole-brain ^{18}F-FDG analysis. The involvement of the vPMC in DLB, with its known role in sensorimotor processing and motor planning lends additional support to the hypothesis that PH is associated with deficits in sensorimotor integration, as experimentally revealed by robot-induced PH in healthy participants (Blanke et al., 2014) and PD patients (Bernasconi et al., 2021). These observations also suggest that specific brain networks are involved in PH, irrespective of their putative origin and thus independent of whether PH are caused by a focal brain lesion, focal epileptic discharge, neurodegenerative disease, or sensorimotor stimulation-induced PH in healthy participants. However, no involvement of the posterior region of the PH-network was found, suggesting that PH in DLB does not involve the pSTS. The pSTS, however, was found to be involved in PD patients with PH, as resting state fMRI revealed decreased functional connectivity between the inferior frontal gyrus and pSTS. pSTS may thus be differently affected regarding PH in DLB and PD. However, we note that there are several differences between both datasets next to etiology (i.e. methods: fMRI versus PET/SPECT; demographics). Moreover, the brain mechanism of symptomatic PH may also differ from robot-induced PH. One hypothesis is that whereas PD pathology in patients with PH would involve the pSTS (Bernasconi et al., 2021), the present data suggest that DLB may not recruit pSTS, but instead recruit more superior parietal regions, as suggested by the present whole-brain analysis (see Fig. 1). Further work is needed to investigate these questions.

Regarding the lateralization of the present results, we postulate that a more pronounced disrupted connectivity on the left-sided PH-network might be related to a more marked hypometabolism in left fronto-

Table 3
Interregional correlation analysis (IRCA) seeding from vPMC in PH + and PH-

BA	Anatomical Label		k	Peak voxelMNI coordinate x	y	z	T
	PH+						
	Midbrain		171	0	−30	−12	−11.2
	Caudate nucleus	R	170	20	16	12	17.6
	Caudate nucleus	L	69	−16	12	8	10.2
	PH-						
	Cerebellum 8	R	565	24	−68	−56	4.9
	Cerebellum 8	L	114	−30	−64	−56	3.9
10, 11, 9, 46, 8, 6, 44, 32	Superior frontal, Middle frontal, Medial frontal, Inferior frontal, Precentral, Postcentral, Anterior cingulate	L/R	8921	−52	0	30	12.5
40	Supramarginal, Superior temporal	R	329	60	−28	38	4.6
6	Precentral,Postcentral	R	519	54	−4	40	7.1
5, 39, 7, 19	Postcentral,Inferior parietal,Superior parietal,Precuneus, Superior occipital	L	2266	−26	−60	62	7
7	Superior parietal	R	407	32	−56	56	6
40	Posterior inferior parietal	L	126	−46	−42	54	5.1
21, 22	Superior temporal, Middle temporal	R	168	60	−16	−4	5.6
21, 22	Middle temporal, Superior temporal	L	368	−60	−16	−10	4.8

Significant clusters observed during IRCA using left ventral premotor cortex (vPMC) as a seed region for PH + and PH- patients. Positive and negative correlations are listed, following positive and negative T-score. Statistical threshold uncorrected $p < 0.001$, $k = 50$ voxels. X Y Z – stereotactic coordinates in MNI space; T – SPM T-score; BA – Brodmann area, k – cluster size in voxels.

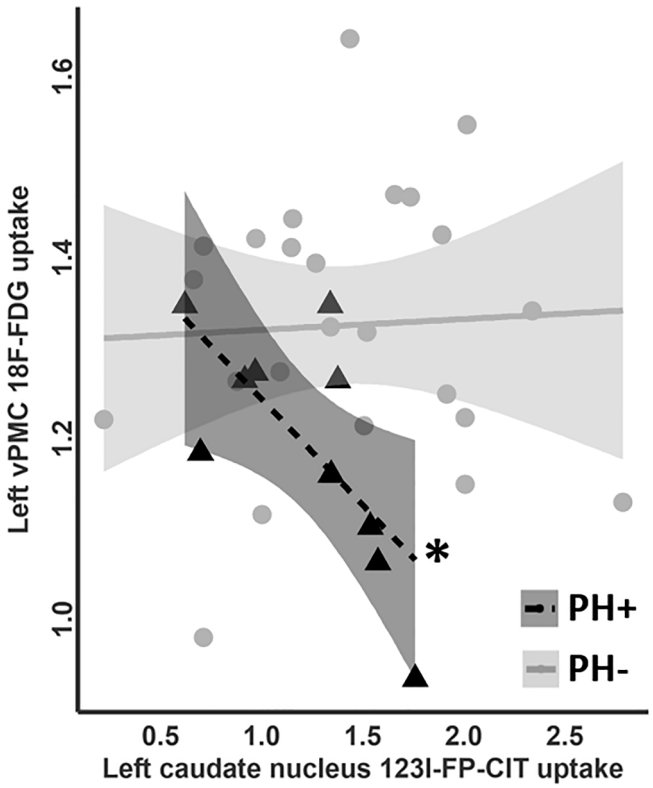

Fig. 4. Correlation analysis between the left vPMC ^{18}F-FDG uptake and the left caudate nucleus ^{123}I-FP-CIT uptake. Pearson correlation between ^{18}F-FDG uptake in the left ventral premotor cortex (vPMC) and ^{123}I-FP-CIT uptake in the left caudate nucleus for PH + patients (black triangles) and PH- (grey dots). *p < 0.05.

parietal areas, at least in the present PH + DLB subjects. In epileptic subjects with PH, these symptoms were usually associated with unilateral brain interference (right or left) (Blanke et al., 2014). In our DLB cohort, subjects observed a presence either behind (n = 3) or on one side (n = 7). For those experiencing the presence on one side, this could be either left (n = 1), right (n = 2), or both (n = 4). Therefore, a more global and bilateral disruption of the PH-network seems more likely in DLB, at variance with a more circumscribed and lateralized impairment in patients with focal lesions. This is somewhat in line with a recent publication about PH in patients with schizophrenia using the same PH-network, showing a disruption of bilateral IFG and right pMTG connectivity (Stripeikyte et al., 2021).

Several hypotheses have been put forward to explain the co-occurrence of pH and VH in neurodegenerative conditions. As they are particularly prevalent in PD and DLB, a role of cortical alpha-synuclein deposition has been evoked. Using a large cohort of autopsy-confirmed DLB cases, Ballard *et al.* observed that VH and delusions were particularly present in DLB subjects with higher Lewy body staging and that VH were associated with less severe tangle pathology (i.e. concomitant AD pathology)(Ballard et al., 2004). Grey matter loss in parietooccipital regions (e.g. inferior occipital and fusiform, lingual and supramarginal gyri) were associated with VH in DLB and PD with dementia. To a lesser extent, inferior frontal and orbitofrontal were also involved (Sanchez-Castaneda et al., 2010; Watanabe et al., 2013). PD subjects with minor hallucinations (PH, passage hallucinations and illusions) showed reduced brain volume in supramarginal and angular, as well as in middle occipital and fusiform gyri (Bejr-Kasem et al., 2019). In addition, widespread reductions in glucose metabolism have been observed in dorsolateral frontal, middle frontal, orbitofrontal, anterior, posterior cingulate, cuneus, and temporooccipital cortex in DLB subjects with VH (Perneczky et al., 2008; Heitz et al., 2015; Morbelli et al., 2019). Our present findings suggest that while a reduced fronto-parietal metabolism is observed in PH + DLB subjects, no significant hypometabolism was observed for VH + subjects. However, we further investigated whether VH in our patients differentially recruited the PH-network. For this purpose, we performed additional network analysis based on the occurrence of VH. These showed that changes of the PH-network in vPMC were limited to patients with PH, as the metabolism neither of vPMC, nor of any other node of the PH-network differed between both VH-groups, suggesting that PH involve vPMC or fronto-parietal cortex, whereas changes for VH predominate in posterior brain regions with less impairment of frontal cortex (Pezzoli et al., 2017).

Using IRCA with the left vPMC of the PH-network as a seed, we showed that PH + lacked the extensive cortical connectivity pattern with frontal, temporal and parietal areas observed for PH- patients. This further confirms a central role of the PH-network (especially vPMC) and its connectivity in relationship to PH. We note that this differential connectivity patterns of vPMC between PH + and PH- patients is compatible with decreased functional connectivity between frontal and posterior cortical regions (parietal and temporal cortex) that have been observed in PD patients with PH and has been more generally associated with outcome processing of sensorimotor signals and the forward model (Blakemore and Frith, 2003; Frith, 2005). The present connectivity data thus link PH in DLB to the hallucination disconnection model, which is a general framework that associates hallucinations with a disruption of frontal communication with posterior brain regions (Friston, 1998; Friston et al., 2016).

Regarding subcortical function, IRCA analysis showed that premotor-striatal connectivity positively correlated in PH + but was absent in PH- (Fig. 3). This suggests that PH are also related to alterations of fronto-striatal connectivity, in line with previous work showing

fronto-striatal impairments associated with VH in PD (Kiferle et al., 2014). While PH + and PH- patients had similar striatal dopaminergic function, we observed a negative correlation between vPMC metabolism and caudate dopaminergic transporter density (Fig. 4) only for PH + patients. This suggests that metabolic alterations in this key region of the PH-related network (left vPMC), are related to striatal dopaminergic changes. Recently, Apostolova et al. showed that reduced glucose metabolism in the bilateral medial frontal and anterior cingulate was correlated with presynaptic dopamine transporter uptake in the cognitive part of the striatum in PD (Apostolova et al., 2020). Grey matter loss in basal ganglia was also observed in association with VH, but further studies are required to determine whether this also applies to DLB patients with PH (Pezzoli et al., 2019). Our findings of a negative correlation between vPMC (and striatal) ^{18}F-FDG metabolism and caudate nucleus ^{123}I-FP-CIT dopaminergic uptake seems puzzling, at first glance. However, similar findings were observed by Huber et al., where a more pronounced striatal dopaminergic deficit was correlated with a relative hypermetabolism in the caudate nucleus and limbic regions for DLB subjects (Huber et al., 2020). Therefore, while we demonstrated a reduced metabolism in vPMC and a disruption in fronto-striatal connectivity for DLB subjects with PH, this does not preclude that, in this specific group, the patients with more marked reduction of striatal dopaminergic deficit have an up-regulation of frontal metabolism, possibly to compensate motor difficulties.

The present study has several limitations which should be considered when interpreting our findings. As for most neuroimaging studies, DLB diagnosis is based on clinical criteria and not on neuropathological confirmation. However, we ensured that each subject had clinically probable DLB (progressive cognitive decline and at least two core features), in addition to reduced presynaptic dopamine transporter imaging and a typical DLB pattern of posterior ^{18}F-FDG hypometabolism (Imamura et al., 1997; Okamura et al., 2001; Gilman et al., 2005). While the retrospective nature of the study can be considered as an advantage for diagnostic confirmation, the attribution of patients as PH + and PH- relied on data available in the medical file. While these symptoms have been thoroughly collected during the initial neurological evaluation leading to PET/SPECT imaging and the diagnosis of probable DLB, they were not assessed using a standardised questionnaire. Moreover, PH and other hallucinations occur spontaneously, vary within and across patients, and may not be reported due to fear of stigmatization (Ffytche et al., 2017; Bernasconi et al., 2021). We thus cannot exclude potential misattribution. Moreover, due to the relatively small sample, ^{18}F-FDG group comparisons were performed with an uncorrected statistical threshold at the cluster level. However, we used an extent threshold of at least 50 voxels for cluster significance. We further note that structural brain MRI images were not available for all included subjects, which could have potentially improved co-registration of ^{18}F-FDG PET scans. Additionally, the analysed ^{18}F-FDG PET images represented average (static) metabolism over a scanning time thus we could not delineate temporal metabolic fluctuations related to the PH-network which would have given more insight about possible alterations related to PH. We also note that the brain mechanisms of pH in DLB, PD, or other neurological aetiologies (i.e. epilepsy, brain tumor) may also differ in some aspects. Future work should investigate the behavioural sensitivity to robot-induced PH in DLB patients in comparisons to other neurological conditions and healthy controls.

5. Conclusions

In summary, the present study advances the neuroscientific understanding of pH in DLB, by revealing fronto-parietal metabolic changes and especially alterations of the vPMC, a key hub in an independently defined PH-network that has also been shown to be altered in patients with PD. In addition, our work revealed that reduced vPMC ^{18}F-FDG uptake was associated with decreased glucose metabolism in widespread cortical regions. Another important finding revealed the involvement of striatal function, showing that PH are additionally associated with alterations in fronto-striatal connectivity. Sensorimotor processes involving premotor cortex and fronto-striatal connectivity are at play for PH in DLB. While VH are rather related to more prominent disruption of posterior brain regions, the present study suggests that PH pathophysiology is compatible with neurocognitive hallucination models that associate a disruption of frontal communication with a specific PH-network(Heitz et al., 2015);(Pezzoli et al., 2017). Future studies should investigate the sensitivity of different patients with dementia to robot-induced PH and acquire functional and structural MRI to corroborate the potential of symptomatic and robot-induced PH in the understanding and diagnosis of psychosis across neurodegenerative diseases.

CRediT authorship contribution statement

Nicolas Nicastro: Conceptualization, Methodology, Formal analysis, Software. **:** . **Giedre Stripeikyte:** Conceptualization, Methodology, Formal analysis, Software. **Frédéric Assal:** Investigation, Writing - review & editing. **Valentina Garibotto:** Investigation, Writing - review & editing. **Olaf Blanke:** Conceptualization, Methodology, Supervision, Writing - review & editing.

Declaration of Competing Interest

The authors declare that they have no known competing financial interests or personal relationships that could have appeared to influence the work reported in this paper.

Acknowledgements

None.

Funding Sources

N. Nicastro: none.
G. Stripeikyte: none.
F. Assal: none.
V. Garibotto: has received grants from the Swiss National Research Foundation (SNF 320030_169876 and 320030_185028) and from the Velux Foundation (project 1123). (none related to the present study)
O. Blanke: has received grants from the Bertarelli Foundation (grant number 532024) and Swiss National Science Foundation (grant number 3100A0-112493) (not related to the present study)

Appendix A. Supplementary data

Supplementary data to this article can be found online at https://doi.org/10.1016/j.nicl.2021.102791.

References

Vann Jones, S.A., O'Brien, J.T., 2014. The prevalence and incidence of dementia with Lewy bodies: a systematic review of population and clinical studies. Psychol Med 44 (4), 673–683.

McKeith, I.G., Boeve, B.F., Dickson, D.W., Halliday, G., Taylor, J.P., Weintraub, D., Aarsland, D., Galvin, J., Attems, J., Ballard, C.G., Bayston, A., Beach, T.G., Blanc, F., Bohnen, N., Bonanni, L., Bras, J., Brundin, P., Burn, D., Chen-Plotkin, A., Duda, J.E., El-Agnaf, O., Feldman, H., Ferman, T.J., Ffytche, D., Fujishiro, H., Galasko, D., Goldman, J.G., Gomperts, S.N., Graff-Radford, N.R., Honig, L.S., Iranzo, A., Kantarci, K., Kaufer, D., Kukull, W., Lee, V.M.Y., Leverenz, J.B., Lewis, S., Lippa, C., Lunde, A., Masellis, M., Masliah, E., McLean, P., Mollenhauer, B., Montine, T.J., Moreno, E., Mori, E., Murray, M., O'Brien, J.T., Orimo, S., Postuma, R.B., Ramaswamy, S., Ross, O.A., Salmon, D.P., Singleton, A., Taylor, A., Thomas, A., Tiraboschi, P., Toledo, J.B., Trojanowski, J.Q., Tsuang, D., Walker, Z., Yamada, M., Kosaka, K., 2017. Diagnosis and management of dementia with Lewy bodies: Fourth consensus report of the DLB Consortium. Neurology 89 (1), 88–100.

Gomperts, S.N., 2016. Lewy Body Dementias: Dementia With Lewy Bodies and Parkinson Disease Dementia. Continuum (Minneap Minn) 22 (2 Dementia), 435–463.

Mosimann, U.P., Rowan, E.N., Partington, C.E., Collerton, D., Littlewood, E., O'Brien, J. T., Burn, D.J., McKeith, I.G., 2006. Characteristics of visual hallucinations in Parkinson disease dementia and dementia with lewy bodies. Am J Geriatr Psychiatry 14 (2), 153–160.
Sala, A., Caminiti, S.P., Iaccarino, L., Beretta, L., Iannaccone, S., Magnani, G., Padovani, A., Ferini-Strambi, L., Perani, D., 2019. Vulnerability of multiple large-scale brain networks in dementia with Lewy bodies. Hum Brain Mapp 40 (15), 4537–4550.
Morbelli, S., Chincarini, A., Brendel, M., Rominger, A., Bruffaerts, R., Vandenberghe, R., Kramberger, M.G., Trost, M., Garibotto, V., Nicastro, N., Frisoni, G.B., Lemstra, A.W., van der Zande, J., Pilotto, A., Padovani, A., Garcia-Ptacek, S., Savitcheva, I., Ochoa-Figueroa, M.A., Davidsson, A., Camacho, V., Peira, E., Arnaldi, D., Bauckneht, M., Pardini, M., Sambuceti, G., Aarsland, D., Nobili, F., 2019. Metabolic patterns across core features in dementia with lewy bodies. Ann Neurol 85 (5), 715–725.
Imamura, T., Ishii, K., Hirono, N., Hashimoto, M., Tanimukai, S., Kazuai, H., Hanihara, T., Sasaki, M., Mori, E., 1999. Visual hallucinations and regional cerebral metabolism in dementia with Lewy bodies (DLB). Neuroreport 10 (9), 1903–1907.
O'Brien, J.T., Firbank, M.J., Mosimann, U.P., Burn, D.J., McKeith, I.G., 2005. Change in perfusion, hallucinations and fluctuations in consciousness in dementia with Lewy bodies. Psychiatry Res 139 (2), 79–88.
Perneczky, R., Drzezga, A., Boecker, H., Forstl, H., Kurz, A., Haussermann, P., 2008. Cerebral metabolic dysfunction in patients with dementia with Lewy bodies and visual hallucinations. Dement Geriatr Cogn Disord 25 (6), 531–538.
Ballard, C., Holmes, C., McKeith, I., Neill, D., O'Brien, J., Cairns, N., Lantos, P., Perry, E., Ince, P., Perry, R., 1999. Psychiatric morbidity in dementia with Lewy bodies: a prospective clinical and neuropathological comparative study with Alzheimer's disease. Am J Psychiatry 156 (7), 1039–1045.
Nagahama, Y., Okina, T., Suzuki, N., Matsuda, M., Fukao, K., Murai, T., 2007. Classification of psychotic symptoms in dementia with Lewy bodies. Am J Geriatr Psychiatry 15 (11), 961–967.
Nagahama, Y., Okina, T., Suzuki, N., Matsuda, M., 2010. Neural correlates of psychotic symptoms in dementia with Lewy bodies. Brain 133 (2), 557–567.
Nicastro, N., Eger, A.F., Assal, F., Garibotto, V., 2020. Feeling of presence in dementia with Lewy bodies is related to reduced left frontoparietal metabolism. Brain Imaging Behav 14 (4), 1199–1207.
Lopez, C., Halje, P., Blanke, O., 2008. Body ownership and embodiment: vestibular and multisensory mechanisms. Neurophysiol Clin 38 (3), 149–161.
Fenelon, G., Soulas, T., Cleret de Langavant, L., Trinkler, I., Bachoud-Levi, A.C., 2011. Feeling of presence in Parkinson's disease. J Neurol Neurosurg Psychiatry 82 (11), 1219–1224.
Lenka, A., Pagonabarraga, J., Pal, P.K., Bejr-Kasem, H., Kulisvesky, J., 2019. Minor hallucinations in Parkinson disease: A subtle symptom with major clinical implications. Neurology 93 (6), 259–266.
Ffytche, D.H., Creese, B., Politis, M., Chaudhuri, K.R., Weintraub, D., Ballard, C., Aarsland, D., 2017. The psychosis spectrum in Parkinson disease. Nat Rev Neurol 13 (2), 81–95.
Wood, R.A., Hopkins, S.A., Moodley, K.K., Chan, D., 2015. Fifty Percent Prevalence of Extracampine Hallucinations in Parkinson's Disease Patients. Front Neurol 6, 263.
Marinus, J., Zhu, K., Marras, C., Aarsland, D., van Hilten, J.J., 2018. Risk factors for non-motor symptoms in Parkinson's disease. Lancet Neurol 17 (6), 559–568.
Arzy, S., Seeck, M., Ortigue, S., Spinelli, L., Blanke, O., 2006. Induction of an illusory shadow person. Nature 443 (7109), 287.
Blanke, O., Pozeg, P., Hara, M., Heydrich, L., Serino, A., Yamamoto, A., Higuchi, T., Salomon, R., Seeck, M., Landis, T., Arzy, S., Herbelin, B., Bleuler, H., Rognini, G., 2014. Neurological and robot-controlled induction of an apparition. Curr Biol 24 (22), 2681–2686.
Bernasconi, F., Blondiaux, E., Potheegadoo, J., Stripeikyte, G., Pagonabarraga, J., Bejr-Kasem, H., Bassolino, M., et al., 2021. Robot-induced hallucinations in Parkinson's disease depend on altered sensorimotor processing in fronto-temporal network. Sci Transl Med 13(591):eabc8362.
A. Varrone, S. Asenbaum, T. Vander Borght, J. Booij, F. Nobili, K. Nagren, J. Darcourt, O. L. Kapucu, K. Tatsch, P. Bartenstein, K. Van Laere, C. European Association of Nuclear Medicine Neuroimaging, EANM procedure guidelines for PET brain imaging using [18F]FDG, version 2, Eur J Nucl Med Mol Imaging 2009; 36(12): 2103-10.
Nicastro, N., Garibotto, V., Poncet, A., Badoud, S., Burkhard, P.R., 2016. Establishing On-Site Reference Values for (123)I-FP-CIT SPECT (DaTSCAN(R)) Using a Cohort of Individuals with Non-Degenerative Conditions. Mol Imaging Biol 18 (2), 302–312.
Borghammer, P., Jonsdottir, K.Y., Cumming, P., Ostergaard, K., Vang, K., Ashkanian, M., Vafaee, M., Iversen, P., Gjedde, A., 2008. Normalization in PET group comparison studies–the importance of a valid reference region. Neuroimage 40 (2), 529–540.
Minoshima, S., Frey, K.A., Foster, N.L., Kuhl, D.E., 1995. Preserved pontine glucose metabolism in Alzheimer disease: a reference region for functional brain image (PET) analysis. J Comput Assist Tomogr 19 (4), 541–547.
Destrieux, C., Fischl, B., Dale, A., Halgren, E., 2010. Automatic parcellation of human cortical gyri and sulci using standard anatomical nomenclature. Neuroimage 53 (1), 1–15.
Faul, F., Erdfelder, E., Lang, A.G., Büchner, A., 2007. G*Power 3: A flexible statistical power analysis program for the social, behavioral, and biomedical sciences. Behav Res Methods 39, 175-191.
Lee, D.S., Kang, H., Kim, H., Park, H., Oh, J.S., Lee, J.S., Lee, M.C., 2008. Metabolic connectivity by interregional correlation analysis using statistical parametric mapping (SPM) and FDG brain PET; methodological development and patterns of metabolic connectivity in adults. Eur J Nucl Med Mol Imaging 35 (9), 1681–1691.
G. Stripeikyte, J. Potheegadoo, P. Progin, G. Rognini, E. Blondiaux, R. Salomon et al. Fronto-temporal disconnection within the presence hallucination network in psychotic patients with passivity experiences. Schizophr Bull 2021; epub ahead of print.
Ballard, C.G., Jacoby, R., Del Ser, T., Khan, M.N., Munoz, D.G., Holmes, C., Nagy, Z., Perry, E.K., Joachim, C., Jaros, E., O'Brien, J.T., Perry, R.H., McKeith, I.G., 2004. Neuropathological substrates of psychiatric symptoms in prospectively studied patients with autopsy-confirmed dementia with lewy bodies. Am J Psychiatry 161 (5), 843–849.
Sanchez-Castaneda, C., Rene, R., Ramirez-Ruiz, B., Campdelacreu, J., Gascon, J., Falcon, C., Calopa, M., Jauma, S., Juncadella, M., Junque, C., 2010. Frontal and associative visual areas related to visual hallucinations in dementia with Lewy bodies and Parkinson's disease with dementia. Mov Disord 25 (5), 615–622.
Watanabe, H., Senda, J., Kato, S., Ito, M., Atsuta, N., Hara, K., Tsuboi, T., Katsuno, M., Nakamura, T., Hirayama, M., Adachi, H., Naganawa, S., Sobue, G., 2013. Cortical and subcortical brain atrophy in Parkinson's disease with visual hallucination. Mov Disord 28 (12), 1732–1736.
Bejr-Kasem, H., Pagonabarraga, J., Martinez-Horta, S., Sampedro, F., Marin-Lahoz, J., Horta-Barba, A., Aracil-Bolanos, I., Perez-Perez, J., Angeles Boti, M., Campolongo, A., Izquierdo, C., Pascual-Sedano, B., Gomez-Anson, B., Kulisevsky, J., 2019. Disruption of the default mode network and its intrinsic functional connectivity underlies minor hallucinations in Parkinson's disease. Mov Disord 34 (1), 78–86.
Heitz, C., Noblet, V., Cretin, B., Philippi, N., Kremer, L., Stackfleth, M., Hubele, F., Armspach, J.P., Namer, I., Blanc, F., 2015. Neural correlates of visual hallucinations in dementia with Lewy bodies. Alzheimers Res Ther 7 (1), 6.
Pezzoli, S., Cagnin, A., Bandmann, O., et al., 2017. Structural and functional neuroimaging of visual hallucinations in Lewy Body Disease: A systematic literature review. Brain Sci 7 (7), 84.
Blakemore, S.J., Frith, C., 2003. Self-awareness and action. Curr Opin Neurobiol 13 (2), 219–224.
Frith, C., 2005. The neural basis of hallucinations and delusions. C R Biol 328 (2), 169–175.
Friston, K., Brown, H.R., Siemerkus, J., Stephan, K.E., 2016. The dysconnection hypothesis. Schizophr Res 176 (2–3), 83–94.
Friston, K.J., 1998. The disconnection hypothesis. Schizophr Res 30 (2), 115–125.
Kiferle, L., Ceravolo, R., Giuntini, M., Linsalata, G., Puccini, G., Volterrani, D., Bonuccelli, U., 2014. Caudate dopaminergic denervation and visual hallucinations: evidence from a (1)(2)(3)I-FP-CIT SPECT study. Parkinsonism Relat Disord 20 (7), 761–765.
Apostolova, I., Lange, C., Frings, L., Klutmann, S., Meyer, P.T., Buchert, R., 2020. Nigrostriatal Degeneration in the Cognitive Part of the Striatum in Parkinson Disease Is Associated With Frontomedial Hypometabolism. Clin Nucl Med 45 (2), 95–99.
Pezzoli, S., Cagnin, A., Antonini, A., Venneri, A., 2019. Frontal and subcortical contribution to visual hallucinations in dementia with Lewy bodies and Parkinson's disease. Postgrad Med 131 (7), 509–522.
Huber, M., Beyer, L., Prix, C., Schonecker, S., Palleis, C., Rauchmann, B.S., Morbelli, S., Chincarini, A., Bruffaerts, R., Vandenberghe, R., Van Laere, K., Kramberger, M.G., Trost, M., Grmek, M., Garibotto, V., Nicastro, N., Frisoni, G.B., Lemstra, A.W., van der Zande, J., Pilotto, A., Padovani, A., Garcia-Ptacek, S., Savitcheva, I., Ochoa-Figueroa, M.A., Davidsson, A., Camacho, V., Peira, E., Arnaldi, D., Bauckneht, M., Pardini, M., Sambuceti, G., Voglein, J., Schnabel, J., Unterrainer, M., Perneczky, R., Pogarell, O., Buerger, K., Catak, C., Bartenstein, P., Cumming, P., Ewers, M., Danek, A., Levin, J., Aarsland, D., Nobili, F., Rominger, A., Brendel, M., 2020. Metabolic Correlates of Dopaminergic Loss in Dementia with Lewy Bodies. Mov Disord 35 (4), 595–605.
Imamura, T., Ishii, K., Sasaki, M., Kitagaki, H., Yamaji, S., Hirono, N., Shimomura, T., Hashimoto, M., Tanimukai, S., Kazui, H., Mori, E., 1997. Regional cerebral glucose metabolism in dementia with Lewy bodies and Alzheimer's disease: a comparative study using positron emission tomography. Neurosci Lett 235 (1–2), 49–52.
Okamura, N., Arai, H., Higuchi, M., Tashiro, M., Matsui, T., Hu, X.S., Takeda, A., Itoh, M., Sasaki, H., 2001. [18F]FDG-PET study in dementia with Lewy bodies and Alzheimer's disease. Prog Neuropsychopharmacol Biol Psychiatry 25 (2), 447–456.
Gilman, S., Koeppe, R.A., Little, R., An, H., Junck, L., Giordani, B., Persad, C., Heumann, M., Wernette, K., 2005. Differentiation of Alzheimer's disease from dementia with Lewy bodies utilizing positron emission tomography with [18F] fluorodeoxyglucose and neuropsychological testing. Exp Neurol 191 (Suppl 1), S95–S103.